https://doi.org/10.1016/j.scib.2023.04.025

Assessing Climatic Impact on Transition from Neanderthal to Anatomically Modern Human Population on Iberian Peninsula: a Macroscopic Perspective

Konstantin Klein[1], Gerd-Christian Weniger[2], Patrick Ludwig[3], Christian Stepanek[4], Xu Zhang[5], Christian Wegener[1] and Yaping Shao[1*]

[1]Institute for Geophysics and Meteorology, University of Cologne, Albertus-Magnus-Platz 1, Cologne, 50923, Germany.
[2]Institute of Prehistory, University of Cologne, Albertus-Magnus-Platz 1, Cologne, 50923, Germany.
[3]Institute of Meteorology and Climate Research, Karlsruhe Institute of Technology, Wolfgang-Gaede-Strasse 1, Karlsruhe, 76131, Germany.
[4]Paleoclimate Dynamics, Alfred Wegener Institute, Helmholtz Centre for Polar and Marine Research, Am Handelshafen 12, Bremerhaven, 27570, Germany.
[5]Alpine Paleoecology and Human Adaption Group, State Key Laboratory of Tibetan Plateau Earth System,Chinese Academy of Sciences, No. 16 Lincui Road, Chaoyang District, Beijing, 100101, China.
[1*]Institute for Geophysics and Meteorology, University of Cologne, Albertus-Magnus-Platz 1, Cologne, 50923, Germany.

*Corresponding author(s). E-mail(s): yshao@uni-koeln.de; Contributing authors: konstantin.klein@uni-koeln.de; wenigerg@uni-koeln.de; patrick.ludwig@kit.edu; Christian.Stepanek@awi.de; xu.zhang@itpcas.ac.cn; cwegener1@uni-koeln.de;

https://doi.org/10.1016/j.scib.2023.04.025

Abstract

The Iberian Peninsula is of particular interest for the Neanderthal (NEA) to anatomically modern human (AMH) population transition. The AMHs arrived in Iberia last from eastern Europe and thus any possible contacts between the two populations occurred here later than elsewhere. The transition process took place in the earlier part of the Marine Isotope Stage 3 ($\sim$ 60-27 ka cal BP) as repeated and profound climate changes challenged the population stability. To investigate how climate change and population interactions influenced the transition, we combine climate data with archaeological-site data to reconstruct the Human Existence Potential, a measure of the probability of human existence, for both the NEA and AMH populations in the Greenland Interstadial 11-10 (GI11-10) and Stadial 10-9/Heinrich event 4 (GS10-9/HE4) times. It is found that during GS10-9/HE4, large parts of the peninsula became unsuitable for NEA human existence and the NEA settlement areas contracted to isolated coastal hot spots. As a consequence, the NEA networks became highly unstable, triggering the final collapse of the population. The AMHs arrived in Iberia in GI10 but were confined to patches in the northern most strip of the peninsula. They were soon facing the much colder climate of GS10-9/HE4, which prevented their further expansion or even caused a contraction of their settlement areas. Thus, due to the constellation of climate change and the dispersal of the two populations into different regions of the peninsula, it is unlikely that the NEAs and AMHs coexisted in extensive areas and the AMHs had a significant influence on the demography of the NEAs.

Keywords: Neanderthals, Aurignacian, Human Existence Potential, Middle to Upper Palaeolithic Transition, Iberia

1 Introduction

The Middle to Upper Palaeolithic population transition in Europe took place between HE5 (Heinrich event 5) and HE4 ($\sim$48-38 ka cal BP), with the indigenous Neanderthal (NEA) population of Middle Palaeolithic (MP) technologies being replaced by the migrating Anatomically Modern Human (AMH) population (for climatological and archaeological timelines see Fig. A12). Due to its geographic location, the Iberian Peninsula is of particular importance for the understanding of this transition, considering that a prolonged survival of the NEAs here has been a subject of debate over the past decades [1–10]. Around 42 $\pm$ 1 ka cal BP, the first AMHs related to the Aurignacian (AUR) techno-complex from eastern Europe reached probably northern Iberia, although small differences in timing between Cantabria and Catalonia cannot be excluded [11]. Their arrival may have coincided with the decline and eventual extinction of the NEAs, but the radiocarbon chronologies of both regions suggest that the MP ended before the arrival of the Aurignacian and only the few sites of the Châtelperronian (CHÂT) techno-complex that end before 40 ka

https://doi.org/10.1016/j.scib.2023.04.025

cal BP [12] may have overlapped with the early Aurignacian [11, 13]. Due to the low resolution of radiometric dating in this time frame and the rapid climate oscillations, the correlation of cultural change and climate change is still a challenge.

Genome sequencing and paleoanthropological analyses indicate that contact and interbreeding between NEAs and AMHs took place in Southwestern Asia and Eastern Europe [14–16], but it is unclear whether such interactions occurred in Iberia and why the NEAs became extinct, i.e., whether the extinction was attributed to abrupt climate change [17], competitive exclusion [18], repeated migration by random species drift [19], inbreeding, allee effects and stochasticity [20] or interbreeding with AMHs [21], low efficiency in exploiting resources of the NEAs in comparison with the AMHs [22] or changes of available biomass [13]. The argument of "cognitive superiority" of the AMHs, which was favoured for decades, is now considered to be the least probable [23]. After decades of research, this pan-European population transition is still not well understood and subject to numerous and often contradictory hypotheses [23].

The Middle to Upper Palaeolithic population transition in Iberia was accompanied by major climate changes on millennial scales during the Marine Isotope Stage 3 (MIS3, $\sim$ 60-27 ka cal BP). Climate proxies from the geological archives in and around Iberia [e.g., peatbogs of Padul and Navarrés [24], speleothems of El Pindal Cave or Eagle Cave [25, 26], marine sediments off the west coast of Portugal or from the Alborán Sea [27–30], lake sediment [31] and pollen records [32]], loess stratigraphy [33] and climate model simulations [34–36], have all revealed strong climate changes on the peninsula during the MIS3 (and MIS2). These changes occurred in correspondence with the Greenland Interstadial (GI) and Stadial (GS) cycles punctuated by Heinrich events and Daansgard-Oeschger events. In stadial times, climate in Iberia was also colder and drier. Pollen data [32] suggest that, with respect to today's climate, the mean annual temperature in the Mediterranean realm was about 5°C lower during the Last Glacial Maximum (LGM) and the mean annual precipitation was less by between 650 mm in north-western and 100 mm in south-eastern Iberia. During the HEs, it had even lower temperatures and drier conditions compared to the LGM [31]. This is also reflected in other geological archives [24–26, 28–30]. [37] found that the SSTs of the North Atlantic during the HE4 dropped by 3 to 6°C in the annual mean and 6 to 10°C in summer and winter, respectively.

In accordance with the time scale of the population transition and the low resolution of radiometric dating, we divide the time domain ($\sim 48-38$ ka cal BP) into three periods. The early period ($\sim$48-43 ka cal BP) comprised HE5, GI12 and GS12, when only the NEAs lived on the peninsular. The middle period ($\sim$43-41 ka cal BP) was a warm phase, comprising GI11 and GI10, interrupted only shortly by GS11 that lasted a few hundred years around 42 ka cal BP. In this period, the NEAs might still be in existence, as the AMHs reached the northern part of Iberia. The late period was a prolonged cold phase of almost 3000 years ($\sim$41-38 ka cal BP), consisting of GS10 and GS9/HE4, interrupted

https://doi.org/10.1016/j.scib.2023.04.025

only short by GI9 that lasted about 200 years around 40 ka cal BP. Suppose the NEAs still existed in the GI11-10 period, then the major shift from the GI11-10 warm climate to the GS10-GS9/HE4 cold climate could have profoundly influenced the population transition on the peninsula, as both the NEAs and AMHs faced serious challenges.

Against this complex background, we take a macroscopic approach to examining how climate change impacted on the population transition and whether the NEAs and AMHs could have extensively coexisted. A number of important studies on the transition have been carried out based on the discoveries from archaeological excavations [38–40], but to achieve an overview of the cultural chronology requires the integration of archaeological and climate data [22, 41–43]. Here, we model the Human Existence Potential (HEP) as a measure of the probability of human existence, for both the NEA and AMH populations under the GI11-10 and GS10-9/HE4 conditions. The HEP is estimated using a set of climatic predictors in combination with the presence/absence records of archaeological sites [44, 45]. The climate predictors are derived from a high-resolution regional climate model simulation nested in a global climate model, and the archaeological sites are the latest compilations of the MP and AUR sites. As the AMHs arrived in the northern part of Iberia at the beginning of GI10 ($\sim$41.5 ka cal BP) [46] and were not yet adapted to the local conditions, we include the AUR sites outside Iberia in the HEP computation for the AMHs. The HEP is first simulated using the sites assigned to the first AUR settlement phase ($\sim$42-37 ka cal BP, [45]) - referred to as AUR-P1, and for comparison, it is then simulated using the sites assigned to both the first and second settlement phases of the AUR ($\sim$42-32 ka cal BP) – referred to as AUR-All. In contrast, the NEAs had already lived in Iberia for thousands of years and were well adapted to the local conditions and therefore, we use only the MP sites in Iberia assigned to the MIS3 (see Appendix B) in the HEP calculation for the NEAs [47]. The use of all MP sites is intentional and the justifications and consequences are discussed in Section 2. Two notes need to be made. First, the MP sites cover a large time span, but the temporal resolution of the dating is very poor. The majority ($\sim$ 95%) of the 99 MP sites found were older than GS10-9/HE4, and we assume they existed in the GI11-10 (or similarly) warm climate, not excluding the possibility that they also existed in cold climate. Second, the use of archaeological sites in the HEP model is to provide a statistically meaningful estimate of the adaptive range of the respective population. [44, 45] showed that the overall HEP results do not change substantially when a few sites were added to or removed from the data set, although there are local implications.

We first derive the HEP models for both the NEA and AMH populations in the GI11-10, assuming they were adapted to the warm climate conditions. The same HEP models are then used to compute the HEP for the two populations in the GS10-9/HE4. Based on the spatial patterns of the HEP, we identify the refuges where the two populations could have survived and regions

https://doi.org/10.1016/j.scib.2023.04.025

where contacts between the two populations might have occurred. By comparing the differences in HEP between GI11-10 and GS10-9/HE4, we estimate the climatic impact on the population transition. We show that, based on our analysis, it is unlikely that the NEA and AMH populations coexisted in extensive areas. The results give new impetus to the discussions on the Middle to Upper Palaeolithic population transition in Iberia.

2 Methods and Data

2.1 Human Existence Potential Model

The HEP is estimated using climate and environment data with a logistic regression model, referred to as the HEP model. It is a second-order polynomial of climate variables with modification functions defining the accessibility of resources [44]. To estimate the HEP model coefficients, the human presence and absence records are defined. Human presence (i.e. HEP = 1) is assumed in a site catchment of 20×20 km^2 centred at an archaeological site, following e.g. [48]. Human absence (i.e. HEP = 0) is assumed in areas where human existence is deemed to be impossible. The logistic regression fits the presence/absence records to a selected set of climate predictors. See section 2.4.

The HEP model (Eq. 1) is trained for N = 1000 times, each time with a different randomly selected subset containing 80% of the data in the presence and absence records. The HEP from each training run is evaluated using the remaining 20% of the presence/absence records. The human existence potential Φ is then computed as

$$\Phi = \frac{1}{1000} \sum_{n=1}^{1000} \left\{ 1 + \exp\left[-(\beta_{0n} + \vec{\beta}_n \cdot \vec{p}) \right] \right\}^{-1} \cdot g_1 \cdot g_2, \tag{1}$$

with β_{0n} being the intercept and β_n the fitted coefficients of the nth training run, and $\vec{p}$ being the standardized second-degree bioclimatic predictors.

The functions g_1 and g_2 define the accessibility of regions based on topography [49]. For this purpose, a linear function (Eq. 2) is fitted to the topographical distribution of the sites (Fig. 1), whereby both the topographical height (g_1) and the roughness (g_2), i.e., the standard deviation of the topography around each site, are included (determined by the mean value and the standard deviation of the 30s topography data set on the grid resolution of the climate data).

$$g_{1\ or\ 2}(x) = \begin{cases} 1.0, & x < x_l \\ 1.0 - (x - x_l) \cdot m, & x_l \le x < x_u \\ 0.8, & x \ge x_u \end{cases} \tag{2}$$

Based on the topographic height distributions shown in Fig. 1, the g_1 parameters for the AMHs are $x_l = 350$ m and $x_u = 2000$ m, and for the NEAs are $x_l = 450$ m and $x_u = 2000$ m. The g_2 parameters for the AMHs are $x_l = 70$ m and $x_u = 400$ m, and as the roughness at the MP sites did not show a clear

https://doi.org/10.1016/j.scib.2023.04.025

pattern, this is not considered for the accessibility calculation. Furthermore, the sea level is assumed to be 90 m lower than today's and all grid points lying below the sea level are masked out.

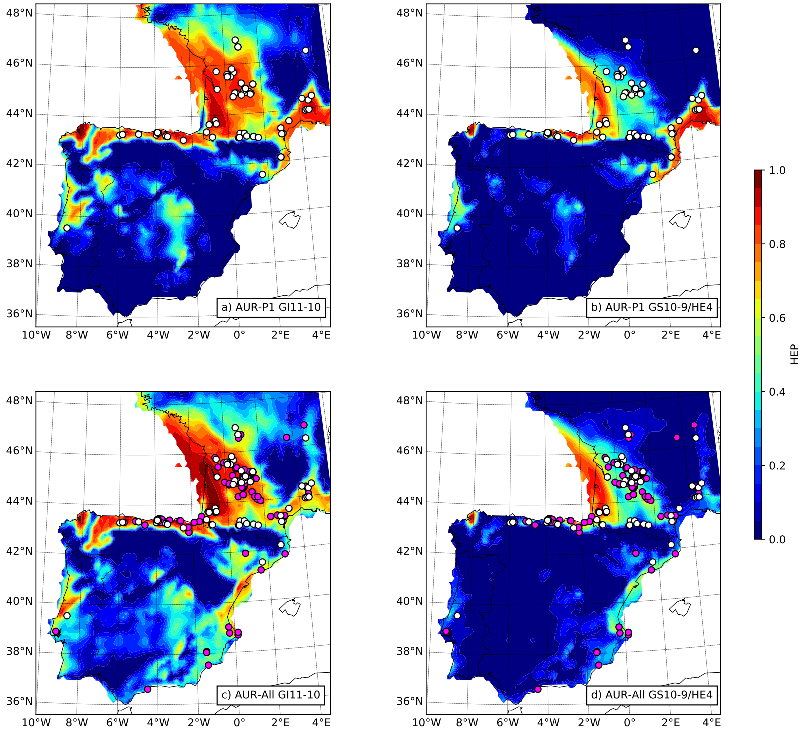

Fig. 1 (a) Topographic height distribution of the archaeological sites of AUR-All and MP; (b) as (a), but for the standard deviation of topography around the site, namely, the roughness.

2.2 Archaeological Data

The MP archaeological data set consists of 99 sites with proofs of NEA existence in Iberia during MIS3 (white squares in Fig. 3), as listed in Table S1. Most of the sites are securely dated and assigned to the Mousterian techno-complex. Seven of these sites show evidence of another techno-complex in a sublayer of the stratigraphy, the CHÂT. This techno-complex is supposed to represent a transition phase from the Middle Palaeolithic to Upper Palaeolithic. Human fossils found in the CHÂT layers regularly belong to NEAs. Therefore, it can be assumed that NEAs were the makers of the CHÂT, although some researcher doubt this link (for the latest state of the discussion see [12]). All MP sites are included for training the HEP model for the NEA population, although some of the sites might no longer be inhabited at the time of GI11-10.

https://doi.org/10.1016/j.scib.2023.04.025

We divided the Aurignacian into two phases, AUR-P1 and AUR-P2, which are approximately correlated with the chronological time frames of 43-37 ka cal BP and 37-32 ka cal BP, respectively. This division is debatable, but we opted for this to allow the assignment of the data compiled from the literature to be based on typological attributions and chronometric dates. While in some cases, the assignment of a site is not unambiguous, on the pan-European scale, no significant distortion of the results is expected. For training the HEP model for the AMH population, only the AUR sites located to the south of 47°N and west of 6°E are used. For the AUR-P1, there are 66 sites, and for the AUR-All (AUR-P1 plus AUR-P2), there are 203 sites (dots in Fig. 4). All sites used are listed in Appendix A of [45]. The underlying georeferenced database is online available [50]. Only sites with well-documented, dated or diagnostic assemblages are considered, and the highly disputed ones are excluded from further analysis. Two Aurignacian sites require special attention, the Lapa do Picareiro site and the Cueva de Bajondillo site. For both, the respective excavators postulate their classification in the AUR-P1 [39, 51]. In Cueva de Bajondillo, new radiocarbon dating was carried out on old excavation material. The charcoals give an age of 40.6 - 44.8 ka cal BP for level 13 and have been claimed by the excavators to date an Early Aurignacian but without discussion of the stratigraphic context although they have published in numerous papers since 1997 that this area is disturbed [10]. The lack of diagnostic artefacts in the stone tool inventory also argues against the classification of this site in an Early Aurignacian [52, 53]. This site is therefore not considered further in our analysis. In the case of Lapa do Picareiro, the small stone tool inventory of less than 50 pieces can be assigned to an Aurignacian. However, the early radiocarbon dates all come from the area below or from the lower edge of the find layer. Therefore, it cannot be decided with certainty that they actually date the find context (see also [10]). The Lapa do Picareiro site is preliminary assigned to AUR-P1 and has been placed as a test in the analysis.

2.3 Climate Data

The COSMOS, employed for glacial conditions [54], is used to simulate the GI11-10 and GS10-9/HE4 global climate conditions. For each of the climate simulations, a data set covering 35 model years is created after spinning up the initial coupled atmosphere-ocean state over a time period of 1400 model years. The climate model is integrated at a time resolution of 40 minutes. Climate output is generated by averaging over a period of 6 hours. For both simulations, the boundary conditions are specified to those at 40ka, as described in [55]. In particular, the Earth's orbit is specified with an eccentricity of 0.013146, an obliquity of 23.6126°, and a longitude of the perihelion of 358.167° with respect to the vernal equinox [56]. Concentrations of trace gases are 193 ppm of carbon dioxide, 400 ppb of methane, and 240 ppb of nitrous oxide. To realistically model the GS10-9/HE4 conditions, fresh water release to the North Atlantic [57] is imposed, which attenuates the thermohaline circulation and leads to decreased SST over the North Atlantic and reduced evaporation. The GCM

https://doi.org/10.1016/j.scib.2023.04.025

simulated atmosphere climate data has a T31 spatial resolution of $\sim 3.75°$ with 19 vertical layers. The ocean model, including a thermodynamic sea ice model, employs a bipolar curvilinear model grid with a formal horizontal resolution of $3.0° \times 1.8°$ and 40 unevenly spaced vertical layers.

To increase the horizontal resolution of the climate data for HEP modelling, regional climate simulations are carried out by nesting the Weather Research and Forecasting (WRF) model [58] into the COSMOS runs. The WRF runs for GI11-10 and GS10-9/HE4 last each for 35 years. The first five years of the model run are reserved for the model spin up and thus only the results for the last 30 years are used for the analysis. The resolution of the innermost domain of the WRF simulation is 0.15°, approximately 12.5 km, and the high resolution is achieved through a two-step nesting, i.e., COSMOS-T31 → WRF-50 km → WRF-12.5 km. The domain of the WRF-50 km run covers the entire Europe, while the domain of the WRF-12.5 km run focuses on southwest Europe (Fig. A1).

The land ice cover data for the WRF runs are taken from reconstructions by the ICE-6G-C model of the PMIP4 database [59]. For the GI11-10 run, the ice cover is assumed to arise from a sea level of -72 m (relative to today's sea level), and for the GS10-9/HE4 run to arise from a sea level of -96 m. The vegetation is set as [60]. The topography over the ice sheet as well as the coastline are also adapted based on the respective ICE-6G-C reconstructions used for GI11-10 and GS10-9/HE4. The same orbital parameters and trace gas concentrations as set in the COSMOS model are used in the WRF model for consistency. A more detailed description on how the WRF-model can be adjusted to perform regional paleoclimate simulations can be found in [34, 35].

2.4 Predictor Selection

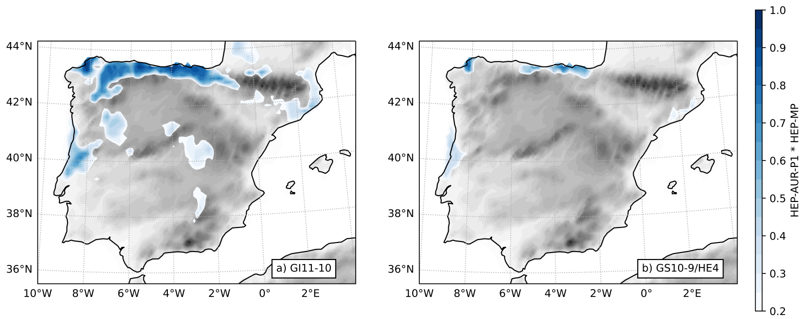

Fig. 2 Dendrogram correlation cluster of the bioclimatic variables for (a, top) GI11-10 and (b, bottom) GS10-9/HE4 and separation of the variables into the groups of mean temperature (green), temperature seasonality (red), daily temperature variation (blue), mean precipitation (magenta), precipitation seasonality (yellow) and mean dryness (cyan).

https://doi.org/10.1016/j.scib.2023.04.025

Seventeen bioclimatic variables (as listed in Tab. 1) are computed from the WRF simulated climate data [44], from which a subset is chosen as predictors for the HEP model. For both GI11-10 and GS10-9/HE4, the same combination of predictors is used. The collinearity of the 17 bioclimatic variables is

Table 1 Definition and clusters of the 17 bioclimatic variables considered as the candidate predictors of the HEP.

Cluster	Bioclim Var	Definition
Mean temp.	Bio1	Annual Mean Temp.
(T-mean)	Bio5	Max Temp. of Warmest Month
	Bio6	Min Temp. of Coldest Month
	Bio10	Mean Temp. of Warmest Quarter
	Bio11	Mean Temp. of Coldest Quarter
Temp. seasonality	Bio4	Temp. seasonality
(T-var)	Bio7	Temp. Annual Range
Daily temp. variation	Bio2	Mean Diurnal Range
	Bio3	Isothermality
Mean precip.	Bio12	Annual Precip.
(P-mean)	Bio13	Precip. of Wettest Month
	Bio16	Precip. of Wettest Quarter
	Bio19	Precip. of Coldest Quarter
Precip. seasonality	Bio14	Precip. of Driest Month
(P-var)	Bio15	Precip. Seasonality
Mean dryness	Bio17	Precip. of Driest Quarter
(D-mean)	Bio18	Precip. of Warmest Quarter

first evaluated (1) to reduce the number of predictors, and (2) to preclude the collinearity between the predictors, which may falsify the logistic regression [61, 62]. The collinearity is examined using a hierarchical clustering of the distance matrix ($\boldsymbol{D} = 1 - \boldsymbol{R}$ with $\boldsymbol{R}$ being the correlation matrix), or a dendrogram. To do this, variable clusters are hierarchically combined until one last cluster is left. The degree of independence among the clusters is measured using the distance score. As Fig. 2 shows, the dendrogram subdivides the bioclimatic variables into six clusters of collinear variables, as listed in Table 1.
Permuting the variables from the six clusters gives 400 combinations, thus the number of variables to be used as predictors must be significantly reduced. Bio2 and Bio3 are first excluded, as they vary on a time scale much shorter than the response timescale of humans to climate change. As quarterly rainfall better represents the moisture conditions (for vegetation) than monthly rainfall, Bio13 and Bio14 are excluded. As the variables of the mean temperature cluster are highly correlated, it is sufficient to use Bio1 to represent them. Likewise, Bio4 is selected to represent temperature seasonality. These considerations limit the combinations of predictors to five possibilities: Bio1, Bio4, (Bio12/16/19), Bio15, (Bio17/18). The quarterly rainfall quantities are further limited to either warm/cold or wet/dry quarters, thus eliminating the combinations of Bio1/4/16/15/18 and Bio1/4/19/15/17.
The remaining four combinations are tested for multicollinearity using the VIF (Variance Inflation Factor) analysis (2). For a combination of five variables, a

https://doi.org/10.1016/j.scib.2023.04.025

VIF is calculated for each variable from the coefficients of a linear regression of the variable to the other four. The combination Bio1/4/12/15/17 is excluded because it contains variables with a VIF > 10, a commonly used threshold for multicollinearity [63]. The three remaining combinations Bio1/4/12/15/18, Bio1/4/16/15/17 and Bio1/4/19/15/18 all have VIF < 10, but since they produce very similar HEP estimates (Fig. A2 and A3), we finally select Bio1, 4, 16, 15, 17 as the HEP predictors.

2.5 Statistical Evaluation

Embedded in the HEP estimates, there may be two types of uncertainties. The first is associated with the paleoclimate reconstructions using climate models. A full assessment of this type of uncertainty is beyond the scope of this study, as it must rely on the collective effort of the climate modelling community at large. However, we have used here the state of the art of climate model simulations and through dynamic down scaling to gain high-resolution climate data as has not been done before for studies of human existence. The second is associated with the archaeological data. The HEP model is trained N (= 1000) times, each time with a random selection of 80% of the presence/absence records. The remaining 20% of the records is used to evaluate the model performance. We have also done sensitivity tests and found that by dropping or adding a few archaeological sites, the resulting HEP patterns basically do not change except for areas where the density of archaeological sites is very low. For example, the inclusion of the Lapa do Picareino site in AUR-P1 can somewhat change the HEP pattern near the west coast of Portugal, and for such cases, specific attention needs to be paid to the model outcomes. Discussions on the HEP model performance have been made in [44] and [64]. The two quantities are used for the evaluation of the HEP model, namely, the "area under a receiver operating characteristics curve" (AUC) and the Brier skill score (BSS). The Brier Skill Score (BSS) defined as

$$\mathrm{BSS} \; = \; \frac{1}{N} \sum_{n=1}^{N} \left(1 \; - \; \frac{BS_n}{BS_0} \right)$$

is used as a measure of model goodness. BS_n is the Brier Score [65] for the n-th run, defined as

$$BS_n = \frac{1}{J} \sum_{j=1}^{J} \left(\Phi_{nj} - \Phi_{oj} \right)^2$$

where J is the number of the 20% presence/absence records, Φ_{nj} and Φ_{oj} are the model predicted HEP and the presence/absence record at record j, respectively. BS_0 is the Brier Score of the same run with $\vec{\beta}$ (but not β_0) set to zero in Equation (1). Because for a given training run n, $\Phi_n(\beta_0) = 1/[1 + exp(-\beta_0)]$ is the simplest model, a BSS = 0 implies that the HEP model performance is identical to the simplest model, while a BSS = 1 is

https://doi.org/10.1016/j.scib.2023.04.025

the perfect model meaning that all training runs perfectly reproduce the 20% presence/absence records. A negative BSS is possible, indicating that the HEP model performance is worse than the simplest model. The BSS thus determines the improvement of the regression compared to a reference model in which only the intercept is considered. AUC is another measure of the model goodness. A large AUC represents a high rate of correct binary classification by the model by comparing the true positive and false positive rates [66]. Using the N training runs, the model performance is evaluated using BSS and AUC for the different regressions are shown in Tab. 3. Both BSS and AUC values are quite large, showing that the HEP model performance is satisfactory.

Table 2 Variance inflation factor (VIF) of the bioclimatic variables from the mean temperature (T mean), temperature seasonality (T var), mean precipitation (P mean), precipitation seasonality (P var), and mean dryness (D mean) groups. The upper four factors correspond to the GI11-10 and the lower ones to the GS10-9/HE4 climate.

	T mean	T var	P mean	P var	D mean
1/4/12/15/17	5.26	1.74	**10.22**	6.54	**13.39**
1/4/12/15/18	5.37	1.78	5.24	5.63	4.49
1/4/16/15/17	5.19	1.75	3.85	6.42	6.49
1/4/19/15/18	5.32	1.76	2.05	5.63	2.47
1/4/12/15/17	6.94	2.14	8.25	8.29	$mathbf{12.35}$
1/4/12/15/18	7.4	2.16	4.63	7.56	5.29
1/4/16/15/17	6.86	2.17	2.99	8.26	6.33
1/4/19/15/18	7.21	2.14	1.67	7.74	3.1

Table 3 Area under a receiver operating characteristics curve (AUC) and Brier skill score (BSS) for the logistic regression shown in Fig. 3 and 4.

	MP	AUR-All	AUR-P1
AUC	0.89 ± 0.011	0.88 ± 0.013	0.9 ± 0.014
BSS	0.78 ± 0.01	0.78 ± 0.01	0.78 ± 0.015

3 Results and Discussions

Fig. 3 shows the HEP for the NEA population under the conditions of GI11-10 and GS10-9/HE4. In GI11-10 (Fig. 3a), high-HEP regions existed in coastal areas and parts of the northern Meseta, where most MP sites are located. The areas along the north coast, the Mediterranean coast and the west coast of Portugal had the highest HEP with values exceeding 0.9, i.e., the NEA existence in these areas was very likely.

In contrast, north-western Iberia and southern Meseta had low HEP, i.e., the NEA existence in these areas was very unlikely. This result is consistent with the archaeological site distribution, as no MP sites are found here. Both Mesetas have a rich data record with numerous surface sites of the Middle Pleistocene. However, dated sites from the late Middle Palaeolithic are rare.

https://doi.org/10.1016/j.scib.2023.04.025

The absence could therefore possibly be a research gap. But long-term surveys in the western part of northern Meseta (e.g. in the Duero Basin) confirm that the absence of sites there is not due to research bias but might indicate abandonment of the area after MIS5 [67]. Although a high-HEP region, the northern Meseta shows human settlement only in its eastern part, while the western part was uninhabited. Against this backdrop, the two regions might have acted as a climate barrier which separated the high-HEP region of the west coast of Portugal from the rest of high-HEP regions on the peninsula, making the exchanges between the NEA groups during MIS3 difficult.
The NEAs were well adapted to all terrains. The mountain ranges in central Iberia, including the Iberian System (Sistema Ibérico) and Central System (Sistema Central), which appeared to be obstacles for the AMHs to expand into central Iberia (Fig. 4a), were potential habitats for the NEAs. The adaptation of the NEAs to the various conditions on the peninsula is seen in the broad frequency distribution of the topographic features (Fig. 1) and local-climatic conditions (Fig. A4) of the MP sites. The diverse local-climatic conditions are reflected in the range of annual mean temperature (Bio1) and precipitation seasonality (Bio15). The distributions of the precipitation in the wettest (Bio16) and driest (Bio17) quarters show that the NEAs preferred to live in relatively dry areas, although some MP sites *(less than 30%)* are located in regions with more rainfall (Fig. A3 and A9), e.g., the northern coast of Iberia. The broad climate adaptive range of the NEAs implies at the same time the differences between the NEA populations in the north and south of Iberia. However, the NEAs were generally absent in cold areas (with annual mean temperature Bio1 $<\sim 2°$ C) accompanied by strong seasonal temperature variations (Bio4 $\sim 5°$ C) that were typical for inland Iberia, especially the southern Meseta (Fig. A8).

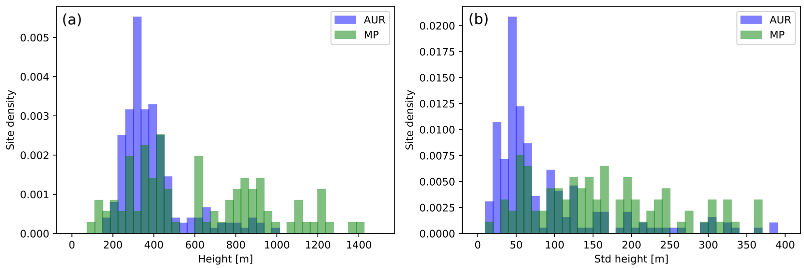

Fig. 3 (a) NEA Human Existence Potential for GI11-10 warm climate, and (b) for GS10-9/HE4 cold climate. White squares mark the MP sites.

During the GS10-9/HE4, the HEP for the NEA population decreased by 0.1 - 0.5 across almost entire Iberia (Fig. 3b). The decrease was more pronounced in the interior than in coastal areas, indicating that the probability of the NEA

https://doi.org/10.1016/j.scib.2023.04.025

existence in the interior of Iberia, which was already small in the GI11-10, further diminished. Several hot spots on the coastal strip retained high HEP values, which could serve as refuges for the NEAs, including the Cantabrian coast, Mediterranean coast centred around the Valencia, Gibraltar area, coast of Portugal, and small areas in the Ebro depression and adjacent northern Meseta. The HEP values in the Portuguese coastal area hardly changed, but the area suitable for the NEA existence was reduced and now surrounded by the low-HEP areas and maintaining networks to the east was almost certainly impossible.

Fig. 4a shows the HEP for the AMH population in GI11-10, obtained from the AUR-P1 experiment. Franco-Cantabria was a high-HEP region where also archaeological sites are densely distributed. In northern Iberia, high-HEP regions extended to the west coast of Spain, much further than Arnero (in Asturias) which is the westernmost site in our data set. Also, the coastal area in northern Portugal and the area to the Central System around Madrid were potentially suitable for settlement. While the Mediterranean France, reaching as far as the south of the Pyrenees, showed high probability of AMH existence, with HEP values ranging from 0.75 to 0.95. It is unlikely that the AMHs of the first AUR phase existed in the rest of in the Mediterranean coastal areas of Spain. The only potential site south of the 40 Latitude is the outlier Lapa do Picareiro. Its assignment to the AUR-P1 is disputed [40].

The AMHs adapted to a narrower topographical range compared to the NEAs. Few sites were found at altitudes higher than 600 m with variations larger than 150 m (Fig. 1). The frequency distributions of the climate variables at the AUR sites indicate that the AMHs were adapted to regions of temperate climate with similar annual mean temperatures and relatively high temperature seasonality. The low HEP values in central and southern Iberia are related to the high annual mean temperatures there (Fig. A4). In comparison to the NEAs, the AMHs lived in more humid areas with relatively low seasonal rainfall variability.

In GS10-9/HE4, the HEP for the AMHs dropped sharply in large parts of the west Mediterranean region (Fig. 4b). The inland of Iberia, which was partly suited for AMH existence in GI11-10, became a hostile area in GS10-9/HE4, with the HEP values falling largely to below 0.05. The decrease occurred also in the coastal areas of Iberia. For example, the coastal areas of Portugal, favourable for AMH existence in GI11-10, almost disappeared completely. Only the Cantabrian coast and the northern most part of the Mediterranean coast retained suitable HEP.

The HEP for the AMHs obtained from the AUR-All experiment for GI11-10 and GS10-9/HE4 are shown in Fig. 4c and d, respectively. A comparison with Fig. 4a and c reveals that the two experiments give similar results, except for the Iberian Mediterranean coast. This important difference is understandable. On the pan-European scale, as reflected in HEP, the AMH population suffered a major setback in GS10-9/HE4, but quickly recovered in the post HE4 period.

https://doi.org/10.1016/j.scib.2023.04.025

There is evidence that the AMHs later adapted to the colder climate conditions and in the post HE4 period started to disperse into previously unsettled colder regions, e.g., northern Europe and British Islands [45]. As the AUR-All experiment takes account of all AUR sites in Europe, implying that the AUR humans existed in more diverse climate conditions, the Iberian Mediterranean coast emerged as a region favourable for the AMH existence.

Derived via a quadratic logistic regression of the archaeological presence/absence records to a set of bio-climatic predictors, HEP represents the probability of human existence, namely, a kinematic statement how likely humans existed at given location and time. At the same time, it is a measure of the potential for human existence of a particular techno-complex under given climate conditions. Regions of high HEP are potentially attractive in the process of human dispersal. Two main conclusions can be drawn from the model results.

First, the GI11-10 to GS10-9/HE4 climate change had a profound detrimental impact on the NEA population. The timing of the NEA extinction in Iberia, as elsewhere, is highly debated [7, 8, 33, 68, 69]. The NEA fossils from El Sidrón are dated directly to 48.4 ± 3.2 ka cal BP [70]. The fragmentary NEA remains from Sima de las Palomas de Cabezo Gordo (likely not preserved in the primary deposition) were found together with burnt fauna bones which give two radiocarbon ages of 42.01 and 38.4 ka cal BP [5, 68]. The radiocarbon dating of bones is less reliable [7], and the stratigraphic context of Units A and B does not exclude their accumulation occurred long after the NEAs disappeared. While sites with dated NEA fossils are rare, sites with MP technology (representing NEA groups in MIS3) are abundant in Iberia [47]. At several of these sites, MP assemblages are dated to younger than 45 ka cal BP, providing evidence for the late survival of the NEAs [68]. In this context, the "Ebro frontier" model has been proposed, which proclaims southern Iberia to be the last refuge of the NEAs, as the Ebro Valley in northwest Spain prevented the southward dispersal of the AMHs [1, 40].

The stratigraphic revaluation of several of these sites and more recent radiocarbon dating in combination with independent age control using U/Th or luminescence methods [7–11, 69–74] changed the narrative. The late MP layers were pushed back by several millennia. Currently, only a few sites remain, which provide indirect evidence for the late survival of the NEAs in southern Iberia, such as Sima de las Palomas de Cabezo Gordo and Cueva Antón in Murcia [5, 68]. At Gorham's cave in Gibraltar, radiocarbon dating of the layers securely linked to the MP, yielded ages older than 43.8 ka cal BP [75]. Recently, the uppermost alluvial deposits with MP imprints at the open-air site of Cardina/Salto de Boi in northern Portugal are luminescence dated to 39.5 ± 1.8 ka [76]. At the same time, presumed late MP sites, e.g., Gruta da Oliveira were recently pushed back for several 10.000 years [10]. These back and forth changes of the dating illustrates the difficulties in assessing the outliers in the archaeological records, especially when considering that different dating methods such as Optically Stimulated Luminescence (OSL) are used

https://doi.org/10.1016/j.scib.2023.04.025

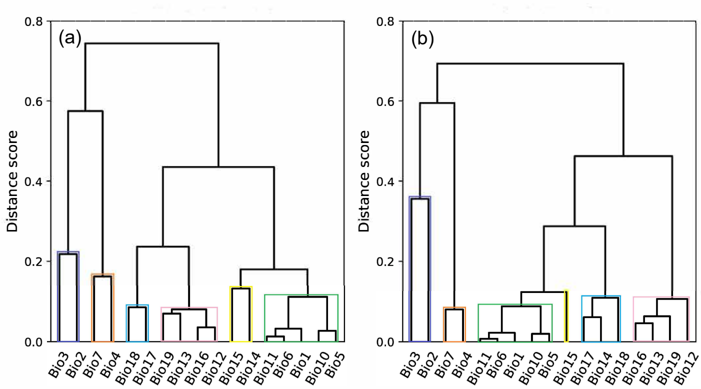

Fig. 4 a) HEP of the AMHs under the GI11-10 and (b) GS10-9/HE4 conditions obtained from the AUR-P1 experiment. (c) and (d), as (a) and (b), but obtained from the AUR-All experiment for comparison.

in addition to the radiocarbon method and different sample materials such as charcoal or bones were dated. Out of nearly 100 MP sites from the MIS3, no more than three might belong to a time span younger than 40 ka cal BP. The vast majority of the sites dated to the Late MP in Iberia suggests an earlier abandonment by the NEAs, probably before ca. 45 ka [70]. This indicates a bust of the NEA population already in HE5 and the final disappearance at the

https://doi.org/10.1016/j.scib.2023.04.025

latest before or during HE4.

The HEP model results provide no additional information on the timing of the NEA extinction, but have shown that if the NEAs survived the HE5 and still existed in the GI10, then the change to the GS10-9/HE4 climate conditions could have had a serious detrimental impact on the NEA population, substantially reducing their living space to isolated hot spots located mainly in coastal areas, and thus breaking up their social networks. The main hot spot in the coastal area of Portugal was cut off from the rest of Iberia by the hostile areas of the Duero Basin in the northwest and the Guadiana and Guadalquivir Basins in the southwest. The Cantabrian coast was only weakly connected to the Mediterranean via the Ebro valley. Between Gibraltar and Murcia, the low HEP indicates that a NEA settlement here was unlikely. The current estimates of the total NEA population in Iberia in GI10 are very uncertain. A preliminary estimate of [77] indicates that the population density during Late MP in central Europe is of the order of 0.0014 Persons per km^2. If this estimate were transferable to the NEAs, then the total NEA population in Iberia would be no more than 500. A model-based study by [78] suggests that the size of the NEA population in Iberia had to be of order of 2000 $\pm$ 1000 humans for population stability. Assuming the population density is proportional to the HEP, we found by integration over the peninsula that the total NEA population that survived in GS10-9/HE4 was about half that in G11-10, probably much below the threshold for population stability. Thus, the challenging climate conditions of GS10-9/HE4 might have two important influences on the NEA population, namely, (1) to reduce the total population on the peninsular to a size below the threshold and (2) to force the NEAs to segregated refuges, which made the networking and mating much more difficult. As a result of these stresses, the remaining NEA population in the refuges might have further declined and finally disappeared.

Second, we do not claim that the initial decay and final disappearance of the NEAs were purely climate driven, but our results show that the demise of the NEAs in Iberia cannot be attributed to the expansion of the AMHs. Compared to the earlier studies on a similar subject [38, 79], this study shows explicitly the high-resolution spatial patterns of human existence in terms of probability and enables a detailed examination of the hypothesis on the late survival of the NEAs. The HEP model results suggest that the hypothesis that southern Iberia served as the last refuge for the NEAs during GS10-9/HE4 [1, 68, 80] needs to be interpreted differently. Fig. 3b shows that the likely NEA refuges in GS10-9/HE4 were the coastal areas. In southern Iberia, regions suitable for the NEA existence with a HEP ¿ 0.5 were confined to the southern tip of Spain, largely cut off from the rest Iberia, and thus southern Iberia was unlikely to be a significant refuge. [35] showed that the southern part of Iberia was strongly affected by aridity during HE1 and hostile for human existence. According to [81], climate conditions on the Iberian Peninsula were similar in HE4 and HE1. At the time of GI10, the AMHs just arrived in northern Spain via southern France and were mostly settled in the Cantabrian coastal areas. Our model

https://doi.org/10.1016/j.scib.2023.04.025

shows that even under the climate conditions of GI11-10, only very limited areas were suitable for the AMHs of the AUR. It is highly likely that the AMH population did not expand southward to cross the Ebro valley at the time, and an "Ebro frontier" thus indeed appears to exist. However, this frontier represents rather the northern boundary of a large territory on the Iberian Peninsula, that was not suitable for AMH existence, than a topographic obstacle for the AMHs to expand further south. This is because the conditions south of the Ebro were generally hostile for the AMH settlement during the first phase of the AUR. Consequently, an AMH settlement south of the Ebro was extremely unlikely. Stable and expanded areas for the first AMHs in Iberia were confined to the Cantabrian coast and the northern most part of the Mediterranean coast near France. In GS9/HE4, the AMH population on the pan-European scale was retreating. Furthermore, the conditions for the existence of the AMHs in Iberia were deteriorated and the few suitable areas for their existence were further reduced. In comparison to the NEA population, the AMH population on the peninsula faced even larger challenges for their origins from the north. This shows that during the entire time period from GI10 to GS10-9/HE4, there was little chance for the southward expansion of the AMHs. Only after GS9/HE4, in the second phase of the AUR, the AMHs headed southward along the coast in today's Valencia and Andalucía, while the interior of Iberian remained to be unsettled (Fig. 4). Our conclusion differs from the statement of [38] that the expansion of the AMHs had not been hindered by the HE4.

The probability of NEA and AHM coexistence is the product of the individual HEPs for the NEA and AHM populations, as Fig. 5 shows for the G11-10 and GS10-9/HE4 periods. In both periods GI11-10 and GS10-9/HE4, the overlap of high-HEP areas for the NEAs and for the AMH pioneers is restricted to a small area in northern Iberia. This in theory opens up the possibility of a side-by-side coexistence during the CHÂT that probably reflects the last phase of the NEAs in northern Iberia. The idea of an immigration of the CHÂT from south-western France after the end of the MP [12, 46] brings the question of multiple population breakdowns into the discussion. This spatial restriction of the CHÂT to a limited area in northern and north-eastern Iberia might indicate the difficulties of the dispersal to the rest of the peninsula. Note that the majority of stratigraphic sequences at the end of the MP show a settlement gap towards the AUR, and in the potential contact areas of the two species, sterile layers may occur between the two occupation phases [8, 82–84]. This means that these sites were probably already abandoned by the NEAs before the AMHs arrived. It is also important to note that there is not a single known site on the Iberian Peninsula that shows an inter-stratification of the Aurignacian with the MP/CHÂT [9]. This would argue against the coexistence of NEA and AMH also in Portugal. Nevertheless, we have included Lapa do Picareiro in our AUR-P1 dataset to test the remote possibility of NEA and AMH coexistence in the coastal areas of Portugal (Fig. 4a, b). In case the dating of Lapa

https://doi.org/10.1016/j.scib.2023.04.025

do Picareiro is confirmed by further analysis [39], this would change the settlement history of the Aurignacian in Iberia and imply that the spread of the AMHs might be relevant to the extinction of the NEAs and the transition from the Middle to Upper Palaeolithic on the Iberian Peninsula. In this case, both species could have inhabited some parts of the peninsula at the same time and the contact between them was more likely.

However, from a macroscopic point of view, this region was separated from all other regions of high AMH existence probability. The pan-European scale model simulation of the Aurignacian dispersal and the high-resolution simulation of Aurignacian dispersal on the Iberian Peninsula both concluded that it is unlikely that the AMHs of the Aurignacian reached the west coast of Portugal in the first settlement phase [64].
If the Lapa do Picareiro site is excluded from the AUR-P1 data set, then the HEP of the AMHs under the GI11-10 and GS10-9/HE4 conditions are as shown in Fig. A5. A comparison with Fig. 4 shows that, as expected, the probability for AHM existence along the western coast of Portugal is reduced under the conditions of both GI11-10 and GS10-9/HE4. Interestingly, even with the Lapa do Picareiro site excluded, there existed a potential corridor weakly linking the Lapa do Picareiro area to the Franco-Cantabria region via the western part of Spain. This suggests that the Aurignacian human settlement at the Lapa do Picareiro site was not impossible, although an event of small probability. The probability of NEA and AHM coexistence, with the Lapa do Picareiro site excluded from the AUR-P1 data set is as shown in Fig. A6.

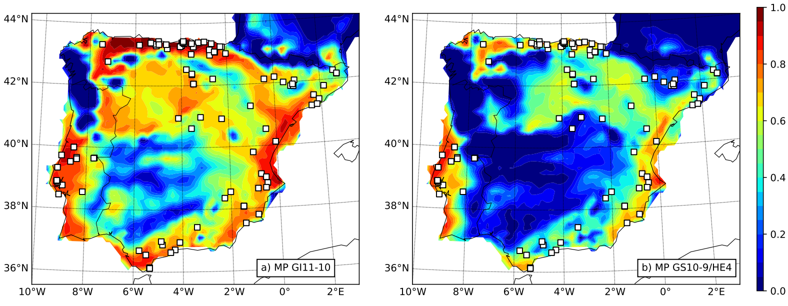

Fig. 5 (a) Probability of NEA and AHM coexistence for G11-10; (b) as (a), but for GS10-9/HE4.

4 Conclusions

Our conclusion based on a macroscopic integration of climate and archaeological site data is that the probability is small for the NEAs and AMHs to compete for resources and existence space. Hence it is unlikely that the expansion of AHMs triggered the extinction of NEAs in Iberia. It is more likely that repeated climate change reduced the HEP for the NEAs to isolated spots

https://doi.org/10.1016/j.scib.2023.04.025

which made it difficult to maintain stable pan-Iberian population networks. This process of deterioration started probably long before GS10-9/HE4, leading to their ultimate extinction.

Overall, the HEP values for the NEAs in GS10-9/HE4 are better than for AMHs. This could be related to the fact that the time span covered of the NEA sites during MIS3 on the Iberian Peninsula is significantly longer than that of the AHMs sites in Iberia. Due to the low resolution of the dating, it is not possible to divide the MP sites into different time slices and we had to included here all MP sites of MIS3 for the statistical evaluation of the NEA adaptation to the Iberian climate/environment conditions. An advantage of doing so is that the conclusions we reached for the NEAs in GI11-10 are transferable to the earlier interstadial times similar to GI11-10, such as GI12. Analogously, the conclusions for the GS10-9/HE4 are transferable to the earlier stadial times, such as HE5. In this context, we can make general statements on the climatic impact on the population transition in Iberia. On the other hand, because of this assumption made, the details of the modelled HEP distributions should be interpreted with caution, as they represent the maximum spread of the NEAs under the given climate. For the future, as dating accuracy continues to increase, it may be useful to calculate HEP for narrower time windows to gain deeper insight into the final phase of NEAs on the Iberian Peninsula.

Supplementary information. This article has no additional supplementary files.

Acknowledgments. This study is funded by the Deutsche Forschungsgemeinschaft (DFG, German Research Foundation) via the Collaborative Research Center 806 (Project ID 57444011). All computations are done at the German Climate Computing Center (DKRZ, Project 965). PL and CS received funding from the Helmholtz Climate Initiative REKLIM. CS acknowledges funding from the Alfred Wegener Institute's research programme "Changing Earth – Sustaining our Future". X.Z. is supported by NSFC BSCTPES project (No. 41988101).

Declarations

- Funding: This study is funded by the Deutsche Forschungsgemeinschaft (DFG, German Research Foundation) via the Collaborative Research Center 806 (CRC 806, Project ID 57444011). All computations are done at the German Climate Computing Center (DKRZ) within Project 965. PL and CS received funding from the Helmholtz Climate Initiative REKLIM. CS acknowledges funding from the Alfred Wegener Institute's research programme "Changing Earth – Sustaining our Future". X.Z. is supported by NSFC BSCTPES project (No. 41988101).
- There is no conflict of interest/Competing interests
- Ethics approval: N.A.
- Consent to participate: All participates agree with the content of the paper

https://doi.org/10.1016/j.scib.2023.04.025

- Consent for publication: All participates agree with the publication of the paper
- Availability of data and materials: Archaeological site data, climate model data and Human Existence Potential estimates are available at request by email to the corresponding author.
- Code availability: code can be shared subject to the DFG intellectual property guidelines
- Authors' contributions: K. Klein, G.-C. Weniger and Y. Shao conceptualised the study; K. Klein, C. Wegener and Y. Shao developed the HEP model; K. Klein and C. Wegener carried out the HEP simulations and analysis under the supervision of Y. Shao and G.-C. Weniger; G.-C. Weniger provided archaeological site data; P. Ludwig carried out the regional climate model simulation and provided data for the HEP simulations; C. Stepanek and X. Zhang carried out the global climate model simulations and provided data for the regional climate model. K. Klein and Y. Shao drafted the paper, K. Klein, C. Wegener and P. Ludwig prepared the graphs, and all co-authors contributed to the improvement of the manuscript.

References

[1] Zilhão, J. The Ebro Frontier: a model for the late extinction of Iberian Neanderthals. *Neanderthals on the edge: 150th Anniversary Conference of the Forbes' Quarry discovery* 111–121 (2000) .

[2] Vaquero, M. El tránsito paleolítico medio/superior en la península ibérica y la frontera del ebro. comentario a zilhão (2006). *Pyrenae* 107–129 (2006) .

[3] Finlayson, C. & Carrión, J. S. Rapid ecological turnover and its impact on neanderthal and other human populations. *Trends in Ecology & Evolution* **22** (4), 213–222 (2007). URL https://www.sciencedirect.com/science/article/pii/S0169534707000353. https://doi.org/https://doi.org/10.1016/j.tree.2007.02.001 .

[4] Sepulchre, P. *et al.* H4 abrupt event and late Neanderthal presence in Iberia. *Earth and Planetary Science Letters* **258** (1-2), 283–292 (2007). URL https://linkinghub.elsevier.com/retrieve/pii/S0012821X07002099. https://doi.org/10.1016/j.epsl.2007.03.041 .

[5] Walker, M. J. *et al.* Late Neandertals in Southeastern Iberia: Sima de las Palomas del Cabezo Gordo, Murcia, Spain. *Proceedings of the National Academy of Sciences* **105** (52), 20631–20636 (2008). URL http://www.pnas.org/cgi/doi/10.1073/pnas.0811213106. https://doi.org/10.1073/pnas.0811213106 .

https://doi.org/10.1016/j.scib.2023.04.025

[6] Schmidt, I. *et al.* Rapid climate change and variability of settlement patterns in Iberia during the Late Pleistocene. *Quaternary International* **274**, 179–204 (2012). https://doi.org/https://doi.org/10.1016/j.quaint.2012.01.018 .

[7] Wood, R. E. *et al.* Radiocarbon dating casts doubt on the late chronology of the Middle to Upper Palaeolithic transition in southern Iberia. *Proceedings of the National Academy of Sciences* **110** (8), 2781–2786 (2013). URL http://www.pnas.org/cgi/doi/10.1073/pnas.1207656110. https://doi.org/10.1073/pnas.1207656110 .

[8] Galván, B. *et al.* New evidence of early Neanderthal disappearance in the Iberian Peninsula. *Journal of Human Evolution* **75**, 16–27 (2014). URL https://linkinghub.elsevier.com/retrieve/pii/S0047248414001481. https://doi.org/10.1016/j.jhevol.2014.06.002 .

[9] Kehl, M. *et al.* Towards a revised stratigraphy for the Middle to Upper Palaeolithic boundary at La Güelga (Narciandi, Asturias, Spain). Soil micromorphology and new radiocarbon data. *Boletín Geológico y Minero* **1129** (1-2), 183–206 (2018). URL http://www.igme.es/boletin/2018/129_1/BGM_129-1-2_Art-8.pdf. https://doi.org/10.21701/bolgeomin.129.1.008 .

[10] Zilhão, J. *et al.* A revised, Last Interglacial chronology for the Middle Palaeolithic sequence of Gruta da Oliveira (Almonda karst system, Torres Novas, Portugal). *Quaternary Science Reviews* **258**, 106885 (2021). URL https://linkinghub.elsevier.com/retrieve/pii/S0277379121000925. https://doi.org/10.1016/j.quascirev.2021.106885 .

[11] Wood, R. *et al.* El Castillo (Cantabria, northern Iberia) and the Transitional Aurignacian: Using radiocarbon dating to assess site taphonomy. *Quaternary International* **474**, 56–70 (2018). URL https://linkinghub.elsevier.com/retrieve/pii/S1040618215300720. https://doi.org/10.1016/j.quaint.2016.03.005 .

[12] Rios-Garaizar, J. *et al.* The intrusive nature of the châtelperronian in the iberian peninsula. *PLOS ONE* **17** (3), 1–18 (2022). URL https://doi.org/10.1371/journal.pone.0265219. https://doi.org/10.1371/journal.pone.0265219 .

[13] Vidal-Cordasco, M., Ocio, D., Hickler, T. & Marín-Arroyo, A. Ecosystem productivity affected the spatiotemporal disappearance of neanderthals in iberia. *Nature Ecology & Evolution* **6** (11), 1644–1657 (2022). https://doi.org/https://doi.org/10.1038/s41559-022-01861-5 .

[14] Trinkaus, E. European early modern humans and the fate of the neandertals. *Proceedings of the National Academy of*

https://doi.org/10.1016/j.scib.2023.04.025

Sciences **104** (18), 7367–7372 (2007). URL https://www.pnas.org/content/104/18/7367. https://doi.org/10.1073/pnas.0702214104, https://www.pnas.org/content/104/18/7367.full.pdf .

[15] Fu, Q. *et al.* The genetic history of Ice Age Europe. *Nature* **534** (7606), 200–205 (2016). URL http://www.nature.com/articles/nature17993. https://doi.org/10.1038/nature17993 .

[16] Vallini, L. *et al.* Genetics and Material Culture Support Repeated Expansions into Paleolithic Eurasia from a Population Hub Out of Africa. *Genome Biology and Evolution* **14** (4) (2022). URL https://doi.org/10.1093/gbe/evac045. https://doi.org/10.1093/gbe/evac045, evac045 .

[17] Staubwasser, M. *et al.* Impact of climate change on the transition of Neanderthals to modern humans in Europe. *Proceedings of the National Academy of Sciences* **115** (37), 9116–9121 (2018). URL http://www.pnas.org/lookup/doi/10.1073/pnas.1808647115. https://doi.org/10.1073/pnas.1808647115 .

[18] Banks, W. E. *et al.* Neanderthal Extinction by Competitive Exclusion. *PLoS ONE* **3** (12), e3972 (2008). URL https://dx.plos.org/10.1371/journal.pone.0003972. https://doi.org/10.1371/journal.pone.0003972 .

[19] Kolodny, O. & Feldman, M. W. A parsimonious neutral model suggests Neanderthal replacement was determined by migration and random species drift. *Nature Communications* **8** (1), 1040 (2017). URL http://www.nature.com/articles/s41467-017-01043-z. https://doi.org/10.1038/s41467-017-01043-z .

[20] Vaesen, K., Scherjon, F., Hemerik, L. & Verpoorte, A. Inbreeding, Allee effects and stochasticity might be sufficient to account for Neanderthal extinction. *PLOS ONE* **14** (11), e0225117 (2019). URL https://dx.plos.org/10.1371/journal.pone.0225117. https://doi.org/10.1371/journal.pone.0225117 .

[21] Stringer, C. & Crété, L. Mapping interactions of homo neanderthalensis and homo sapiens from the fossil and genetic records. *PaleoAnthropology* **2022:2**, 401–412 (2022). https://doi.org/https://doi.org/10.48738/2022.iss2.130 .

[22] Timmermann, A. Quantifying the potential causes of Neanderthal extinction: Abrupt climate change versus competition and interbreeding. *Quaternary Science Reviews* **238**, 106331 (2020). URL https://linkinghub.elsevier.com/retrieve/pii/S0277379120302936. https://doi.org/10.1016/j.quascirev.2020.106331 .

https://doi.org/10.1016/j.scib.2023.04.025

[23] Villa, P. & Roebroeks, W. Neandertal demise: An archaeological analysis of the modern human superiority complex. *PLOS ONE* **9** (4), 1–10 (2014). URL https://doi.org/10.1371/journal.pone.0096424. https://doi.org/10.1371/journal.pone.0096424 .

[24] Pons, A. & Reille, M. The holocene- and upper pleistocene pollen record from padul (granada, spain): A new study. *Palaeogeogr. Palaeoclimatol. Palaeoecol.* **66**, 243–263 (1988). URL https://doi.org/10.1016/0031-0182(88)90202-7. https://doi.org/10.1016/0031-0182(88)90202-7 .

[25] Moreno, A. *et al.* A speleothem record of glacial (25-11.6 kyr bp) rapid climatic changes from northern Iberian Peninsula. *Glob. Planet. Change* **71**, 218–231 (2010). https://doi.org/https://doi.org/10.1016/j.gloplacha.2009.10.002 .

[26] Domínguez-Villar, D. *et al.* Early maximum extent of paleoglaciers from Mediterranean mountains during the last glaciation. *Sci. Rep.* **3**, 2034 (2013). https://doi.org/https://doi.org/10.1038/srep02034 .

[27] Lebreiro, S., Moreno, J., McCave, I. & Weaver, P. Evidence for heinrich layers off portugal (tore seamount: 39 °n, 12 °w). *Marine Geology* **131** (1), 47–56 (1996). URL https://www.sciencedirect.com/science/article/pii/0025322795001425. https://doi.org/https://doi.org/10.1016/0025-3227(95)00142-5, ice Rafting and Paleocengraphy of the Northeast Atlantic Ocean Selected papers presented at the 7th European Union of Geosciences .

[28] Naughton, F. *et al.* Climate variability across the last deglaciation in nw iberia and its margin. *Quaternary International* **414**, 9–22 (2016). URL https://www.sciencedirect.com/science/article/pii/S1040618215008514. https://doi.org/https://doi.org/10.1016/j.quaint.2015.08.073 .

[29] Fletcher, W. J. & Sánchez Goñi, M. F. Orbital- and sub-orbital-scale climate impacts on vegetation of the western mediterranean basin over the last 48,000 yr. *Quaternary Research* **70** (3), 451–464 (2008). https://doi.org/10.1016/j.yqres.2008.07.002 .

[30] Combourieu Nebout, N. *et al.* Rapid climatic variability in the west mediterranean during the last 25 000 years from high resolution pollen data. *Climate of the Past* **5** (3), 503–521 (2009). URL https://cp.copernicus.org/articles/5/503/2009/. https://doi.org/10.5194/cp-5-503-2009 .

[31] Moreno, A., González-Sampériz, P., Morellón, M., Valero-Garcés, B. L. & Fletcher, W. J. Northern iberian abrupt climate change dynamics during

https://doi.org/10.1016/j.scib.2023.04.025

the last glacial cycle: A view from lacustrine sediments. *Quaternary Science Reviews* **36** (Complete), 139–153 (2012). https://doi.org/10.1016/j.quascirev.2010.06.031 .

[32] Bartlein, P. J. *et al.* Pollen-based continental climate reconstructions at 6 and 21 ka: a global synthesis. *Climate Dynamics* **37** (3-4), 775–802 (2011). https://doi.org/https://doi.org/10.1007/s00382-010-0904-1 .

[33] Wolf, D. *et al.* Climate deteriorations and Neanderthal demise in interior Iberia. *Scientific Reports* **8** (1), 7048 (2018). URL http://www.nature.com/articles/s41598-018-25343-6. https://doi.org/10.1038/s41598-018-25343-6 .

[34] Ludwig, P., Pinto, J. G., Raible, C. C. & Shao, Y. Impacts of surface boundary conditions on regional climate model simulations of European climate during the Last Glacial Maximum: Regional European Climate During the LGM. *Geophysical Research Letters* **44** (10), 5086–5095 (2017). https://doi.org/https://doi.org/10.1002/2017GL073622 .

[35] Ludwig, P., Shao, Y., Kehl, M. & Weniger, G.-C. The Last Glacial Maximum and Heinrich event I on the Iberian Peninsula: A regional climate modelling study for understanding human settlement patterns. *Global and Planetary Change* **170**, 34 – 47 (2018). https://doi.org/https://doi.org/10.1016/j.gloplacha.2018.08.006 .

[36] Burke, A. *et al.* Risky business: The impact of climate and climate variability on human population dynamics in Western Europe during the Last Glacial Maximum. *Quaternary Science Reviews* **164**, 217 – 229 (2017). https://doi.org/https://doi.org/10.1016/j.quascirev.2017.04.001 .

[37] Rodrigues, T. *et al.* A 1-ma record of sea surface temperature and extreme cooling events in the north atlantic: A perspective from the iberian margin. *Quaternary Science Reviews* **172**, 118–130 (2017). URL https://www.sciencedirect.com/science/article/pii/S027737911630590X. https://doi.org/https://doi.org/10.1016/j.quascirev.2017.07.004 .

[38] d'Errico, F. & Sánchez Goñi, M. F. Neandertal extinction and the millennial scale climatic variability of ois 3. *Quaternary Science Reviews* **22** (8), 769–788 (2003). URL https://www.sciencedirect.com/science/article/pii/S027737910300009X. https://doi.org/https://doi.org/10.1016/S0277-3791(03)00009-X .

[39] Haws, J. A. *et al.* The early aurignacian dispersal of modern humans into westernmost eurasia. *Proceedings of the National Academy of Sciences* **117** (41), 25414–25422 (2020). URL https://www.pnas.org/doi/abs/10.1073/pnas.2016062117. https://doi.org/10.1073/pnas.2016062117, https://www.pnas.org/doi/pdf/10.1073/pnas.2016062117 .

https://doi.org/10.1016/j.scib.2023.04.025

[40] Zilhão, J. The late persistence of the middle palaeolithic and neandertals in iberia: A review of the evidence for and against the ebro frontier model. *Quaternary Science Reviews* **270**, 107098 (2021). URL https://www.sciencedirect.com/science/article/pii/S027737912100305X. https://doi.org/https://doi.org/10.1016/j.quascirev.2021.107098 .

[41] Burke, A. *et al.* The archaeology of climate change: The case for cultural diversity. *Proceedings of the National Academy of Sciences* **118** (30), e2108537118 (2021). URL https://www.pnas.org/doi/abs/10.1073/pnas.2108537118. https://doi.org/10.1073/pnas.2108537118, https://www.pnas.org/doi/pdf/10.1073/pnas.2108537118 .

[42] Beyer, R., Krapp, M., Eriksson, A. & Manica, A. Climatic windows for human migration out of africa in the past 300,000 years. *Nature Communications* **12**, 4889 (2021). https://doi.org/https://doi.org/10.1038/s41467-021-24779-1 .

[43] Timmermann, A. *et al.* Climate effects on archaic human habitats and species successions. *Nature* **604**, 495–501 (2022). https://doi.org/https://doi.org/10.1038/s41586-022-04600-9 .

[44] Klein, K. *et al.* Human existence potential in europe during the last glacial maximum. *Quaternary International* **581-582**, 7–27 (2021). URL https://www.sciencedirect.com/science/article/pii/S1040618220304432. https://doi.org/https://doi.org/10.1016/j.quaint.2020.07.046, the Last Glacial Maximum in Europe - State of the Art in Geoscience and Archaeology .

[45] Shao, Y. *et al.* Human-existence probability of the aurignacian techno-complex under extreme climate conditions. *Quaternary Science Reviews* **263**, 106995 (2021). URL https://www.sciencedirect.com/science/article/pii/S027737912100202X. https://doi.org/https://doi.org/10.1016/j.quascirev.2021.106995 .

[46] Marín-Arroyo, A. B. *et al.* Chronological reassessment of the Middle to Upper Paleolithic transition and Early Upper Paleolithic cultures in Cantabrian Spain. *PLOS ONE* **13** (4), e0194708 (2018). URL https://dx.plos.org/10.1371/journal.pone.0194708. https://doi.org/10.1371/journal.pone.0194708 .

[47] Rotgänger, M. *et al.* Crc806 c1 database iberia late middle palaeolithic to magdalenian (2021).

[48] Becker, D., De Andrés-Herrero, M., Willmes, C., Weniger, G.-C. & Bareth, G. Investigating the influence of different dems on gis-based cost distance modeling for site catchment analysis of prehistoric sites in andalusia. *ISPRS International Journal of Geo-Information* **6** (2) (2017). https://doi.org/10.3390/ijgi6020036 .

https://doi.org/10.1016/j.scib.2023.04.025

[49] Becker, J. J. *et al.* Global Bathymetry and Elevation Data at 30 Arc Seconds Resolution: SRTM30_plus. *Marine Geodesy* **32** (4), 355–371 (2009). URL https://www.tandfonline.com/doi/full/10.1080/01490410903297766. https://doi.org/10.1080/01490410903297766 .

[50] Schmidt, I. Crc806 e1 aur sites database 20210331 (2021). URL https://doi.org/10.5880/SFB806.63.

[51] Cortés-Sánchez, M. *et al.* An early Aurignacian arrival in southwestern Europe. *Nature Ecology & Evolution* **3** (2), 207–212 (2019). URL http://www.nature.com/articles/s41559-018-0753-6. https://doi.org/10.1038/s41559-018-0753-6 .

[52] Anderson, L., Reynolds, N. & Teyssandier, N. No reliable evidence for a very early aurignacian in southern iberia. *Nature Ecology & Evolution* **3** (5), 713–713 (2019) .

[53] de la Peña, P. Dating on its own cannot resolve hominin occupation patterns. *Nature Ecology & Evolution* **3** (5), 712–712 (2019) .

[54] Zhang, X., Lohmann, G., Knorr, G. & Xu, X. Different ocean states and transient characteristics in Last Glacial Maximum simulations and implications for deglaciation. *Climate of the Past* **9** (5), 2319–2333 (2013). URL https://cp.copernicus.org/articles/9/2319/2013/. https://doi.org/10.5194/cp-9-2319-2013 .

[55] Zhang, X. *et al.* Direct astronomical influence on abrupt climate variability. *Nature Geoscience* **14** (11), 819–826 (2021). URL https://www.nature.com/articles/s41561-021-00846-6. https://doi.org/10.1038/s41561-021-00846-6 .

[56] Laskar, J. *et al.* A long-term numerical solution for the insolation quantities of the earth. *Astronomy & Astrophysics* **428** (1), 261–285 (2004). URL https://doi.org/10.1051/0004-6361:20041335. https://doi.org/10.1051/0004-6361:20041335 .

[57] Knorr, G. *et al.* A salty deep ocean as a prerequisite for glacial termination. *Nature Geoscience* **14** (12), 930–936 (2021). URL https://doi.org/10.1038/s41561-021-00857-3. https://doi.org/10.1038/s41561-021-00857-3 .

[58] Skamarock, W. C. *et al.* A Description of the Advanced Research WRF Model Version 4. Tech. Rep., UCAR/NCAR (2019). URL https://opensky.ucar.edu/islandora/object/opensky:2898.

[59] Peltier, W. R., Argus, D. F. & Drummond, R. Space geodesy constrains ice age terminal deglaciation: The global ICE-6G_c (VM5a) model:

https://doi.org/10.1016/j.scib.2023.04.025

Global Glacial Isostatic Adjustment. *Journal of Geophysical Research: Solid Earth* **120** (1), 450–487 (2015). URL http://doi.wiley.com/10.1002/2014JB011176. https://doi.org/10.1002/2014JB011176 .

[60] Ramankutty, N. *et al.* ISLSCP II Potential Natural Vegetation Cover. *ORNL DAAC* (2010). URL https://daac.ornl.gov/cgi-bin/dsviewer.pl?ds_id=961. https://doi.org/https://doi.org/10.3334/ORNLDAAC/961 .

[61] Durbin, J. Testing for Serial Correlation in Least-Squares Regression When Some of the Regressors are Lagged Dependent Variables. *Econometrica* **38** (3), 410 (1970). URL https://www.jstor.org/stable/1909547?origin=crossref. https://doi.org/10.2307/1909547 .

[62] Dormann, C. F. *et al.* Collinearity: a review of methods to deal with it and a simulation study evaluating their performance. *Ecography* **36** (1), 27–46 (2013). https://doi.org/https://doi.org/10.1111/j.1600-0587.2012.07348.x .

[63] Alin, A. Multicollinearity. *Wiley Interdisciplinary Reviews: Computational Statistics* **2** (3), 370–374 (2010). https://doi.org/10.1002/wics.84 .

[64] Shao, Y. *et al.* in *Modelling human dispersal in space and time* (eds Litt, T., Richter, J. & Schäbitz, F.) *The Journey of Modern Humans from Africa to Europe* 148–170 (Schweizerbart Science Publishers, 2021). URL http://www.schweizerbart.de//publications/detail/isbn/9783510655342/Litt_et_al_Eds_The_Journey_of_Modern.

[65] Brier, G. W. Verification of Forecasts expressed in terms of Probability. *Monthly Weather Review* **78** (1), 1–3 (1950). https://doi.org/https://doi.org/10.1175/1520-0493(1950)078⟨0001:VOFEIT⟩2.0.CO;2 .

[66] Hanley, J. A. & McNeil, B. J. The meaning and use of the area under a receiver operating characteristic (ROC) curve. *Radiology* **143** (1), 29–36 (1982). https://doi.org/https://doi.org/10.1148/radiology.143.1.7063747 .

[67] Sánchez Yustos, P. & Diez Martín, F. Dancing to the rhythms of the Pleistocene? Early Middle Paleolithic population dynamics in NW Iberia (Duero Basin and Cantabrian Region). *Quaternary Science Reviews* **121**, 75–88 (2015). URL https://linkinghub.elsevier.com/retrieve/pii/S0277379115002048. https://doi.org/10.1016/j.quascirev.2015.05.005 .

[68] Zilhão, J. *et al.* Precise dating of the Middle-to-Upper Paleolithic transition in Murcia (Spain) supports late Neandertal persistence in Iberia. *Heliyon* **3** (11), e00435 (2017). URL https://linkinghub.elsevier.com/retrieve/pii/S2405844017308642. https://doi.org/10.1016/j.heliyon.2017.

https://doi.org/10.1016/j.scib.2023.04.025

e00435 .

[69] Kehl, M. *et al.* The rock shelter abrigo del molino (segovia, spain) and the timing of the late middle paleolithic in central iberia. *Quaternary Research* **90** (1), 180–200 (2018). https://doi.org/10.1017/qua.2018.13 .

[70] Higham, T. *et al.* The timing and spatiotemporal patterning of Neanderthal disappearance. *Nature* **512** (7514), 306–309 (2014). URL http://www.nature.com/articles/nature13621. https://doi.org/10.1038/nature13621 .

[71] Maroto, J. *et al.* Current issues in late Middle Palaeolithic chronology: New assessments from Northern Iberia. *Quaternary International* **247**, 15–25 (2012). URL https://linkinghub.elsevier.com/retrieve/pii/S1040618211003879. https://doi.org/10.1016/j.quaint.2011.07.007 .

[72] Wood, R. *et al.* The chronology of the earliest Upper Palaeolithic in northern Iberia: New insights from L'Arbreda, Labeko Koba and La Viña. *Journal of Human Evolution* **69**, 91–109 (2014). URL https://linkinghub.elsevier.com/retrieve/pii/S0047248414000335. https://doi.org/10.1016/j.jhevol.2013.12.017 .

[73] Kehl, M. *et al.* Late Neanderthals at Jarama VI (central Iberia)? *Quaternary Research* **80** (2), 218–234 (2013). URL https://www.cambridge.org/core/product/identifier/S0033589400005925/type/journal_article. https://doi.org/10.1016/j.yqres.2013.06.010 .

[74] Cunha, P. *et al.* The Lowermost Tejo River Terrace at Foz do Enxarrique, Portugal: A Palaeoenvironmental Archive from c. 60-35 ka and Its Implications for the Last Neanderthals in Westernmost Iberia. *Quaternary* **2** (1), 3 (2019). URL http://www.mdpi.com/2571-550X/2/1/3. https://doi.org/10.3390/quat2010003 .

[75] Zilhão, J. Chronostratigraphy of the middle-to-upper paleolithic transition in the iberian peninsula. *Pyrenae* **37** (1), 7–84 (2006). URL https://raco.cat/index.php/Pyrenae/article/view/145166 .

[76] Aubry, T. *et al.* Timing of the Middle-to-Upper Palaeolithic transition in the Iberian inland (Cardina-Salto do Boi, Côa Valley, Portugal). *Quaternary Research* **98**, 81–101 (2020). URL https://www.cambridge.org/core/product/identifier/S0033589420000435/type/journal_article. https://doi.org/10.1017/qua.2020.43 .

[77] Schmidt, I. *et al.* Approaching prehistoric demography: proxies, scales and scope of the Cologne Protocol in European contexts. *Philosophical Transactions of the Royal Society B: Biological Sciences* **376** (1816), 20190714 (2021). URL https://royalsocietypublishing.org/doi/10.1098/

rstb.2019.0714. https://doi.org/10.1098/rstb.2019.0714 .

[78] Klein, K. *Simulating Paleolithic human dispersal using Human Existence Potential and constrained random walk model.* Ph.D. thesis, Institute for Geophysics and Meteorology, University of Cologne, Cologne Germany (2022).

[79] Garcia Garriga, J., Martínez, K. & Preysler, J. Neanderthal survival in the north of the iberian peninsula? reflections from a catalan and cantabrian perspective. *Journal of World Prehistory* **25**, 81–121 (2012). https://doi.org/10.1007/s10963-012-9057-y .

[80] Jennings, R., Finlayson, C., Fa, D. & Finlayson, G. Southern iberia as a refuge for the last neanderthal populations. *Journal of Biogeography* **38**, 1873 – 1885 (2011). https://doi.org/10.1111/j.1365-2699.2011.02536.x .

[81] Naughton, F. *et al.* Wet to dry climatic trend in north-western iberia within heinrich events. *Earth and Planetary Science Letters* **284** (3), 329–342 (2009). URL https://www.sciencedirect.com/science/article/pii/S0012821X09002751. https://doi.org/https://doi.org/10.1016/j.epsl.2009.05.001 .

[82] Bradtmöller, M., Pastoors, A., Weninger, B. & Weniger, G.-C. The repeated replacement model - Rapid climate change and population dynamics in Late Pleistocene Europe. *Quaternary International* **247**, 38–49 (2012). https://doi.org/https://doi.org/10.1016/j.quaint.2010.10.015 .

[83] Mallol, C., Hernández, C. M. & Machado, J. The significance of stratigraphic discontinuities in Iberian Middle-to-Upper Palaeolithic transitional sites. *Quaternary International* **275**, 4–13 (2012). URL https://linkinghub.elsevier.com/retrieve/pii/S1040618211004071. https://doi.org/10.1016/j.quaint.2011.07.026 .

[84] Ramos-Muñoz, J. *et al.* The nature and chronology of human occupation at the galerías bajas, from cueva de ardales, malaga, spain. *PLoS ONE* **17**, e0266788 (2022). URL https://doi.org/10.1371/journal.pone.0266788 .

https://doi.org/10.1016/j.scib.2023.04.025

Appendix A Simulation Domain, Climate Maps, HEP Estimates and Climatic-Archaeological Timelines

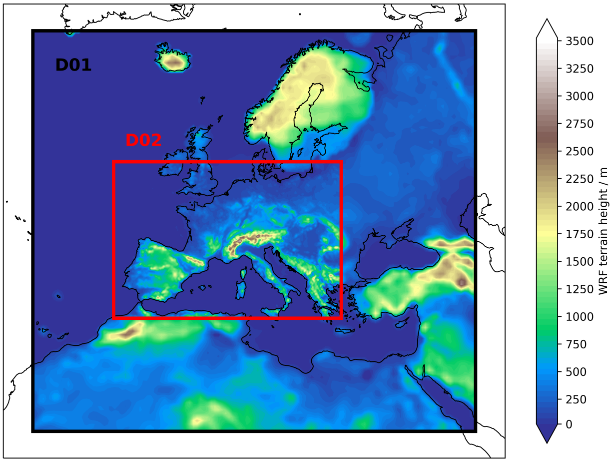

Fig. A1 Two domain WRF setup employed in this study. Domain D01 is driven by climate output produced by the global COSMOS simulation. Shown are geographical location and relative position of outer domain (D01, black box) and inner domain (D02, red box). Shading represents terrain height in WRF. Spatial resolution depends on the domain and is higher in D02 (12.5 km) than in D01 (50 km).

https://doi.org/10.1016/j.scib.2023.04.025

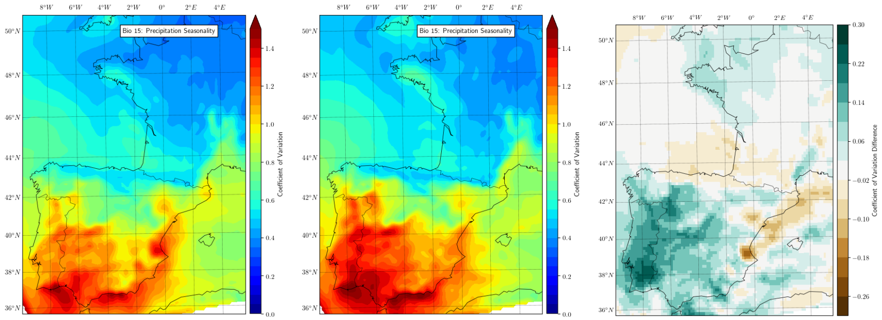

Fig. A2 Precipitation seasonality (Bio15). Left, GI11-10; Middle, GS10-9/HE4; Right, GS10-9/HE4-GI11-10

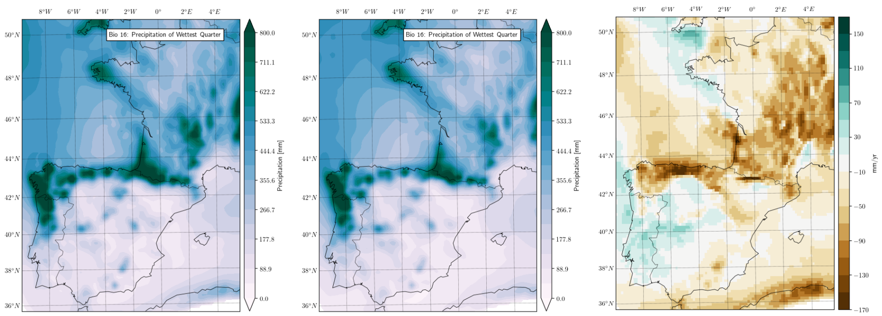

Fig. A3 Precipitation of wettest quarter (Bio16). Left, GI11-10; Middle, GS10-9/HE4; Right, GS10-9/HE4 minus GI11-10

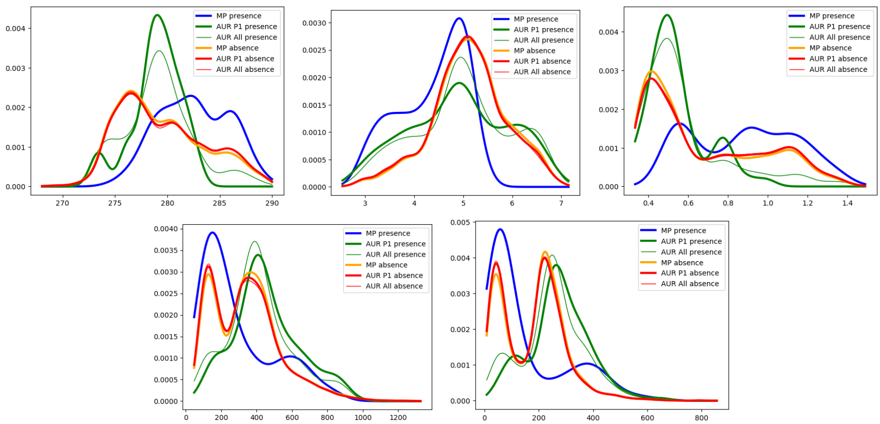

Fig. A4 Climatic conditions (Bio1, Bio4, Bio15, Bio16 and Bio17) at the presence and absence points based on the site distribution of the Aurignacian (AUR-All) and Middle Palaeolithic (MP) techno-complexes for the GI11-10 climate simulation. Human presence is considered in a radius of 20 km around each archaeological site, human absence everywhere else.

https://doi.org/10.1016/j.scib.2023.04.025

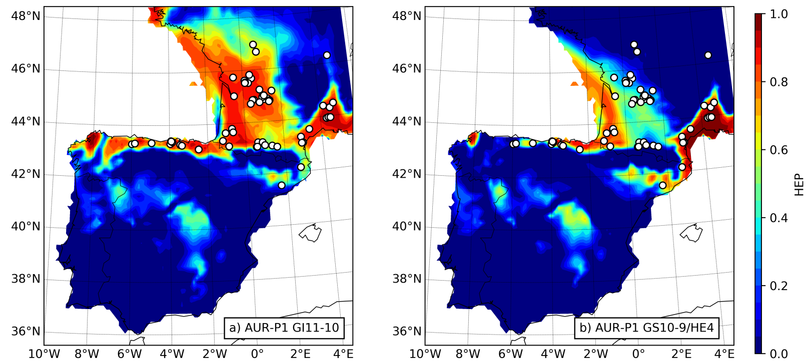

Fig. A5 (a) and (b), as Fig. 4a and b, respectively, but estimated with the Lapa do Picareiro site excluded from the AUR-P1 data set.

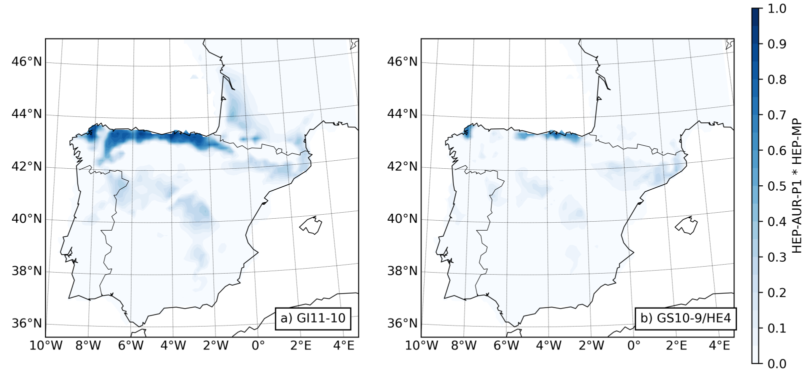

Fig. A6 (a) and (b), as Fig. 5 but with the Lapa do Picareiro site excluded from the AUR-P1 data set.

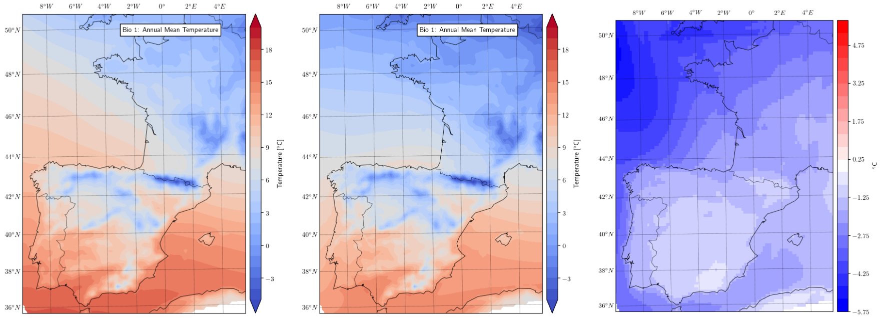

Fig. A7 Annual mean temperature (Bio1). Left, GI11-10; Middle, GS10-9/HE4; Right, GS10-9/HE4-GI11-10

https://doi.org/10.1016/j.scib.2023.04.025

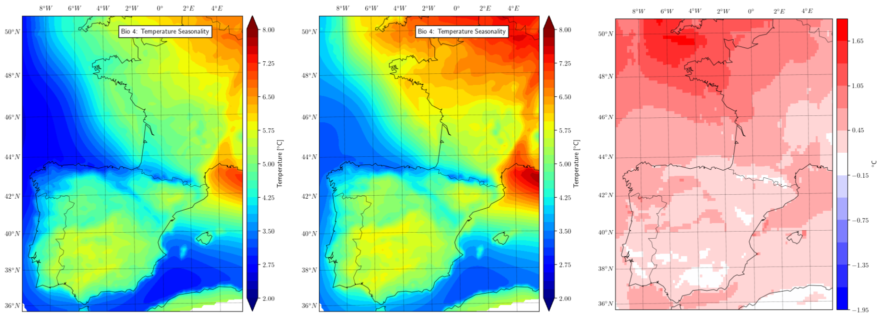

Fig. A8 Temperature seasonality (Bio4). Left, GI11-10; Middle, GS10-9/HE4; Right, GS10-9/HE4-GI11-10

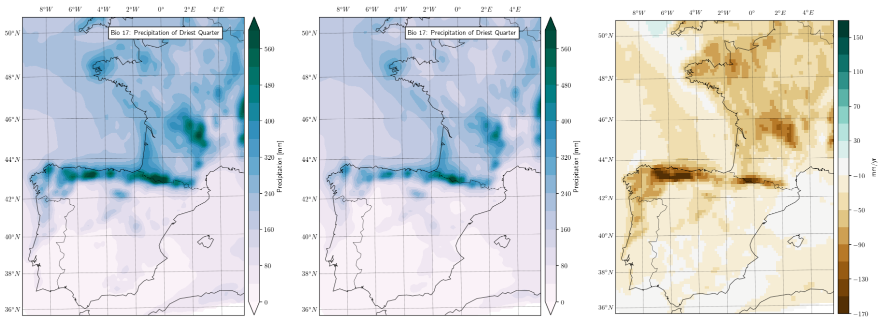

Fig. A9 Precipitation of driest quarter (Bio17). Left, GI11-10; Middle, GS10-9/HE4; Right, GS10-9/HE4 minus GI11-10

https://doi.org/10.1016/j.scib.2023.04.025

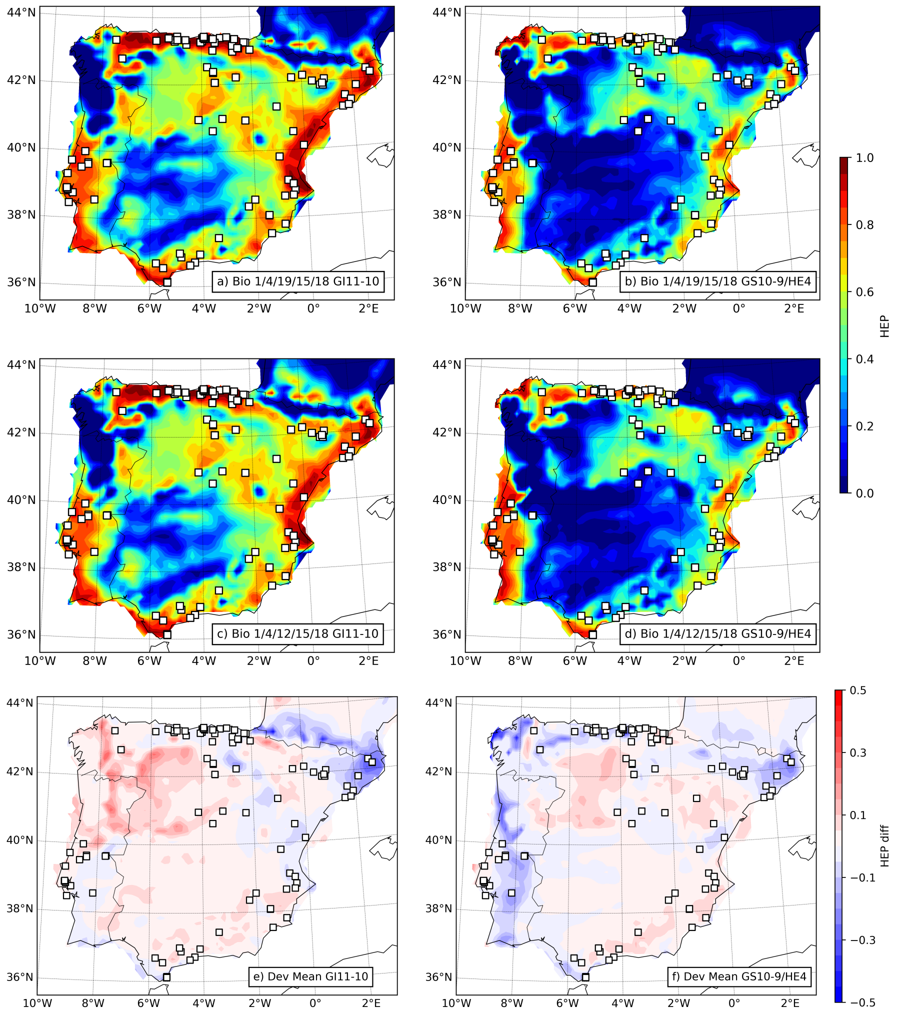

Fig. A10 (a) and (b), MP HEP estimated using bioclimatic variables Bio1/4/19/15/18; (c) and (d) are as (a) and (b), respectively, but estimated using Bio 1/4/12/15/18. (a) and (c) are for GI11-10, and (b) and (d) for GS10-9/HE4. (e) is the deviation of the HEP estimated using Bio1/4/16/15/17 (shown in Fig. 1 of the main text) from the mean of the three estimates for GI11-10; (f) as (e), but for GS10-9/HE4.

https://doi.org/10.1016/j.scib.2023.04.025

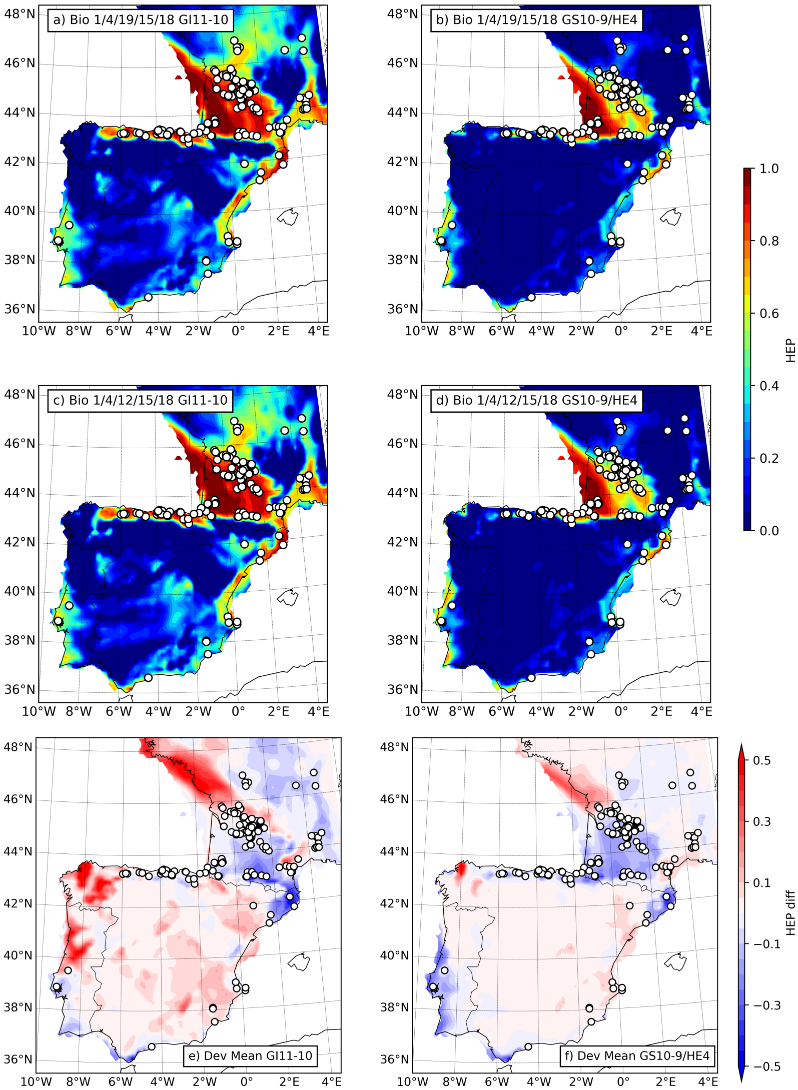

Fig. A11 As Fig. A10, but for AUR-All HEP, i.e., HEP for the Aurignacian techno-complex using all Aurignacian sites.

https://doi.org/10.1016/j.scib.2023.04.025

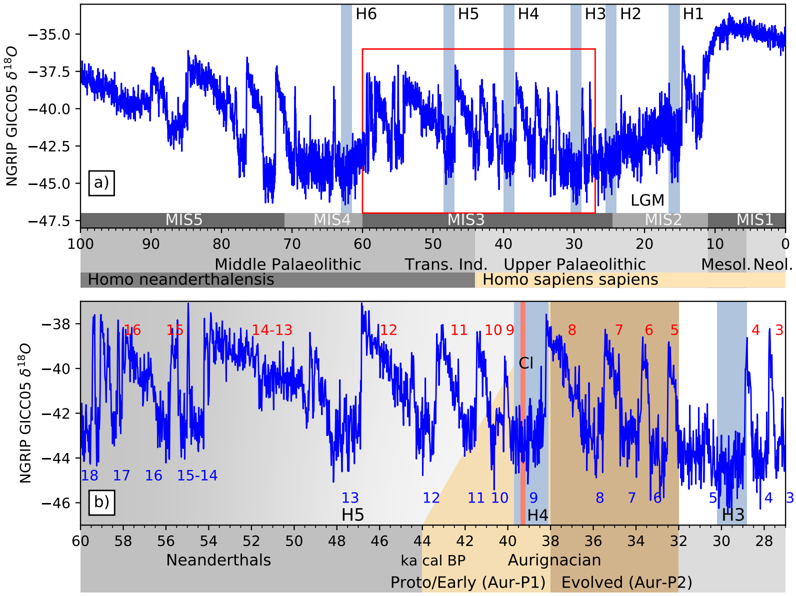

Fig. A12 Climatological and archaeological timelines. The NEAs likely existed in MIS5, MIS4 and the first part of MIS3. The AUR developed in the late half of the Last Glacial Period (LGP). During the LGP, the climate was featured by stadial and interstadial cycles, marked by Heinrich events [H5, H4 etc. labeled in (a)] and Dangsgaard-Oeschger events. In (b), the red numbers mark the Greenland Interstadials (e.g., 10 for GI10), and the blue numbers mark the Greenland Stadials (e.g. 9 for GS9). Isotope δ^{18}O is a surrogate for temperature, with smaller values corresponding to warmer conditions. The abbreviations for the climate timeline include MIS for Marine Isotope Stage, LGM for Last Glacial Maximum, CI for Campanian Ignimbrite volcanic eruption. The abbreviations for the archaeological timeline, referring to the European chronocultural divisions, include Trans. Ind. for Transitional Industries, Mesol. for Mesolithic, and Neol. for Neolithic

https://doi.org/10.1016/j.scib.2023.04.025

Appendix B MP Sites

Table B1: List of the MP and CHÂT sites used in this study, which is an excerpt of the MIS3 MP sites documented in [47]. The CHÂT sites are in italics

Site Name	Site Type
Abauntz	Cave
Abric Romani	Abri
AGP5	Cave
Almonda	Cave
Amalda	Cave
Anton, Cueva	Cave
Arbreda, Cueva de L'	Cave
Ardales, Cueva de	Cave
Arenillas, Covacho de	Unknown
Arrillor Cave	Cave
Axlor (Azlor/Axlor, Cueva de)	Cave
Bajondillo, El	Cave
Beneito, Cueva	Cave
Boja, La	Abri
Buraca Escura	Cave
Buraca Grande	Cave
Caldeirão, Gruta do	Cave
Cantavieja, Cueva de los toros	Cave
Carigüela/Carihuela, Cueva de la	Cave
Casares, Los	Cave
Castillo, El	Cave
Cochino	Cave
Coll Verdaguer, Cova del	Cave
Columbeira	Cave
Conceicáo	Open Air
Conde (Forno), Cueva del	Cave
Covalejos	Cave
Cuco, El	Abri
Dalt del Tossal de la Font, Cova de	Cave
Devil's Tower	Cave
Eirós, Cova	Cave
Ekain	Cave
Ermita, Cueva de la	Cave
Ermitons, Cueva de los	Cave
Escoural 3, Gruta do	Cave
Esquilleu, Cueva del	Cave
Estret de Tragó, Cova del	Cave
Figueira Brava, Gruta da	Cave

https://doi.org/10.1016/j.scib.2023.04.025

Finca Doña Martina	Abri
Flecha, Cueva de la	Cave
Foradada (Calafell, Cova)	Cave
Foz do Enxarrique	Open Air
Fuentes, Las	Unknown
Gegant, Cova del	Cave
Gorham's Cave	Cave
Güelga, La	Cave
Higueral de Valleja Cave	Cave
Higueral-Guardia de Motillas	Cave
Hornos de la Peña	Cave
Hotel California	Open Air
Ibex Cave	Cave
Jarama VI	Cave
Kurtzia	Open Air
Labeko Koba	Cave
Lapa dos Furos	Cave
Lezetxiki	Cave
Llonin Cave	Cave
Millán, Cueva	Cave
Mira Nascente	Open Air
Mirón, El	Cave
Molino, Abrigo del	Abri
Mollet I	Cave
Morín, Cueva	Cave
Moros de Gabasa, Cueva de los	Cave
Muricecs, Cova dels	Cave
Negra, Cova	Cave
Niño, Cueva del	Cave
Oliveira, Gruta da	Cave
Otero, El	Cave
Palomar, El (Albacete)	Abri
Palomas (del Cabezo Gordo), Sima de las	Cave
Pego do Diabo	Cave
Peña Cabra	Abri
Peña Miel	Cave
El Pendo	Cave
Picareiro, Lapa do	Cave
Prado Vargas, Cueva de	Cave
Quebrada, Abrigo de la	Abri
Rexidora Cave	Cave
Roca dels Bous	Abri
Ruso, El	Cave
Salemas quarry	Open Air
Salemas, Gruta de	Cave

https://doi.org/10.1016/j.scib.2023.04.025

Salt, El	Cave
San Cristobal, Fuentes de	Abri
Santa Linya, Cova Gran de	Cave
Santimamiñe, La cueva de	Cave
Sidrón, El	Cave
Sima de las Palomas de Teba	Abri
Sopeña, Abrigo de	Abri
Teixoneres Cave	Cave
Trucho, Fuente del	Cave
Valdegoba	Cave
Valiña, A	Cave
Valle de las Orquideas	Open Air
Vanguard Cave	Cave
Vilas Ruivas	Open Air
Viña, La	Abri
Zafarraya, Cueva del Boquete de	Cave

https://doi.org/10.1016/j.scib.2023.04.025

Appendix C AUR Sites

Table C2: List of the Aurignacan Phase 1 sites used in this study, which is an excerpt of the Aurignacian sites documented in [50].

Abric Romani	Cave
Aurignac II	Cave
Barbas I et III	Open Air
Caminade	Cave
Castanet, Abri	Abri
Cellier, Abri	Abri
Chaise, La	Open Air
Combe Saunière	Cave
Corbiac- Vignoble	Open Air
Covalejos	Cave
Crouzade, La	Cave
Esquicho Grapaou	Cave
Figuier, Grotte du	Cave
Fontéchevade	Cave
Garet	Open Air
Gargas	Cave
Gourdan (El), Grottes de	Cave
Graulet VI, La	Open Air
Labeko Koba	Cave
Laouza, La	Cave
Mandrin, Grotte	Cave
Mas d'Azil, Grotte du	Cave
Otero, Cueva del	Cave
Pair Non Pair	Cave
Pêcheurs	Cave
Picareiro, Lapa do	Cave
Pont Neuf, Le	Cave
Rothschild, Abri	Abri
Souquette, Abri de la	Abri
Tarté	Cave
Traouc de la Fado	Open Air
Tutto de Camayot (La Tuto de Camalhot)	Cave